

Integrated Design and Control of Active Aerodynamic Features for High Performance Electric Vehicles

*Original*

Integrated Design and Control of Active Aerodynamic Features for High Performance Electric Vehicles / Ferraris, A.; De Cupis, D.; de Carvalho Pinheiro, H.; Messana, A.; Sisca, L.; Airale, A. G.; Carello, M.. - In: SAE TECHNICAL PAPER. - ISSN 0148-7191. - ELETTRONICO. - 1:(2021), pp. 1-12. ( 2020 SAE Brasil Congress and Exhibition, BRASILCONG 2020 Sao Paulo (BRASILE) 2020) [10.4271/2020-36-0079].

*Availability:*

This version is available at: 11583/2898056 since: 2021-07-06T10:53:42Z

*Publisher:*

SAE International

*Published*

DOI:10.4271/2020-36-0079

*Terms of use:*

This article is made available under terms and conditions as specified in the corresponding bibliographic description in the repository

*Publisher copyright*

(Article begins on next page)

## Integrated Design and Control of Active Aerodynamic Features for High Performance Electric Vehicles

Alessandro Ferraris, Davide De Cupis, Henrique de Carvalho Pinheiro, Alessandro Messana, Lorenzo Sisca, Andrea Giancarlo Airale and Massimiliana Carello  
Department of Mechanical and Aerospace Engineering, Politecnico di Torino - Italy

### Abstract

Aerodynamics plays a major role on the design of all kinds of vehicles throughout automotive history. Initially the main topic under investigation was the aerodynamic drag reduction to achieve high-energy efficiency, however in the late '60s the vertical aerodynamic forces gained traction, particularly in high performance cars. The automotive market usually treats design, aerodynamics and vehicle dynamics in different departments. This paper proposes an integrated approach for the aerodynamics development in which a sport car is defined as reference vehicle. The objective of the concurrent engineering operation is to control the aerodynamic forces by implementing active surfaces control finally improving vehicle lap time. The vehicle dynamics analysis is carried out in cooperation with vehicle aerodynamics in order to perform the hardware and software design of the active system. The paper presents a case study in which an active aerodynamics control system is designed and successfully simulated numerically, with a co-simulation between MATLAB/Simulink and VI-Grade CarRealTime. The development process of the control system with a fuzzy logic is described and relevant results are presented. Furthermore, to assess the vehicle dynamics improvements, a specific maneuver and a tailored track were developed to highlight the phenomena induced by the active aero surfaces. A final validation, through a static simulator testing session, is performed and presented and the overall conclusions in terms of objective and subjective performance improvements are presented.

### Introduction

The purpose of this paper is to verify if and to what extent it is possible to improve vehicle performance on track by implementing active aerodynamic systems and features [1]. The vehicle dynamics analysis is carried out in continuous cooperation with vehicle aerodynamics analysis, in order to perform, in parallel, the hardware and software design of the active systems.

Active aerodynamics, as vehicle aerodynamics itself, is generally, as a topic, too complex and bounded to the shape of body surfaces to be treated analytically. Aerodynamic surfaces are, in general, developed with the aid of CAD, analyzed with CFD and validated experimentally in wind tunnels. In literature, the topic has been treated in different studies both performed through CFD and wind tunnel testing. One relevant example of this kind of studies can be found in [2], where a CFD analysis of a high-speed car with movable bodywork elements has been performed and transient simulations have been executed. Different phases of flaps opening process, associated to time, has been represented and the time evolution of the vehicle lift coefficient ( $C_L$ ) referred to the flaps' rotation angle and relative time for different flaps' positioning has been reported.

The effects of ride height variations have been also analyzed in detail, dealing with the interaction between air flow through vehicle body and tires, both in race [3] and road cars [4, 5]. Vehicle body shape and position, as well as its mechanical characteristics [6,7], are key design factors.

The aerodynamic transients have been deepened in [8], where a full aerodynamic study has been performed on a prototype vehicle provided of an active wing able to substantially variate its Angle Of Attack (AOA). The

aerodynamic study has been performed both through CFD and wind tunnel test, and through a track test on a real vehicle prototype. Considering the results of this work, it could be stated that up to an actuation frequency of about 2 Hz the AOA variation can be considered quasi-static. This hypothesis will be used in the development of the active systems and the control strategy.

This paper inherits the 4WD (Four Wheel Drive) full electric vehicle model developed in [9-13] and aims to implement an active aerodynamics control strategy through the actuation of two aerodynamic surfaces. The control algorithms' development procedure has been implemented according to an iterative path with an extended use of MaxPerformance package of VI-CarRealTime, in co-simulation with Matlab-Simulink environment.

Specific maneuvers have been developed to test the action of the active control systems in development phase. The control systems operation has been, then, validated on a real track layout as first and, finally, with a static DIL simulator session.

### Vehicle Model and Tailored Maneuvers

All the control algorithms in this paper are developed and validated by using VI-CarRealTime. It operates with a simplified four-wheeled vehicle model and the vehicle is a reduced DOF model including 5 rigid parts and 14 DOF distributed as following:

- 6 DOF for the vehicle chassis (sprung mass);
- 4 DOF for suspensions' stroke;
- 4 DOF for wheels' longitudinal slip.

Suspension and steering system kinematic properties, compliance and component data are described by lookup tables using a conceptual approach. Additional stiffnesses for the suspension components and for the body chassis compliance can be added expanding the model up to 20 DOF. Other vehicle subsystems (brakes and powertrain) are described using differential and algebraic equations, so that no extra part is present in the model. The influence of front and rear ride heights on aerodynamic forces is expressed in the software, as for other parameters already seen, in the form of a lookup table.

The studied model is a 4WD full electric vehicle as presented in [9-13]. It has been modified to match the technical specifications high-end full electric vehicles (such as Rimac C2 or Lotus Evija), and the vehicle dimensions with the reference CAD model used for aerodynamic simulations are shown in Table 1. Table 1

Table 1 - Vehicle reference model technical specification

Parameter	Value	
Vehicle sprung mass	2050	kg
Vehicle un-sprung mass	190	kg
Total maximum power	1257	kW
Wheelbase	2691	mm
CoG longitudinal front wheel distance	1369	mm
CoG height	378	mm
Front track width	1700	mm

Rear track width	1620	mm
Front tires overall radius	352	mm
Rear tires overall radius	364	mm
Frontal area	2,1	m <sup>2</sup>

From the aerodynamic point of view, the reference vehicle body shape selected for this paper is the Aston Martin Vantage 2019, which has been studied from the aerodynamic point of view in [14]. The main assumptions considered in the development of the model are:

- Aerodynamic transients are neglected for an actuation frequency up to 2Hz;
- Different aerodynamic effects are assumed to sum up according to superposition principle;
- Roll and yaw effects on aerodynamic forces are neglected.

With VI-CarRealTime it is possible to simulate both open-loop or closed-loop maneuvers. The latter is made possible by a driver model (the VI-Driver) which is substantially a feed-back controller which actuates the vehicle commands based on two reference signals: the reference trajectory and the reference speed-profile. While the first reference signal is contained in the track file, the second one is computed by the software considering the reference trajectory (which is split in segments roughly corresponding to single corners) and three performance parameters (defined for each trajectory segment):

- Longitudinal acceleration performance;
- Longitudinal braking performance;
- Lateral performance.

The longitudinal performance parameters define a target slope for the speed profile respectively in acceleration and braking, substantially describing how much aggressive the driver will be on accelerator and braking pedal. The lateral performance parameter, instead, defines a target lateral acceleration, effectively providing a reference value for the minimum speed in the corner. VI-CarRealTime provides two types of events able to run lap-time simulations:

- Static lap-time: the user is simply requested to insert manually the three performance parameters, which will define the reference speed profile for each corner;
- MaxPerformance: the user defines (for the whole track) three starting values for performance parameters, an iteration step and a tolerance value in terms of trajectory and speed. The software, then, performs an iterative process repeating the maneuver (each time reducing the performance parameters by the defined iteration step) until the vehicle can complete it without exceeding the tolerance values defined by the user.

Two tailored maneuvers were created in order to effectively develop the control strategy and better highlight the results of the two active aerodynamic aero pack:

- the 'Parabolica'
- the 'GRIP Track'.

### *Parabolica*

This first closed-loop maneuver "Parabolica" has been developed with the aim to verify the operation of active aerodynamics' control systems through the full traveling of a medium-high speed corner (Figure 1). The width of the track is constant and equal to 10 m for the whole track length, the slope is null.

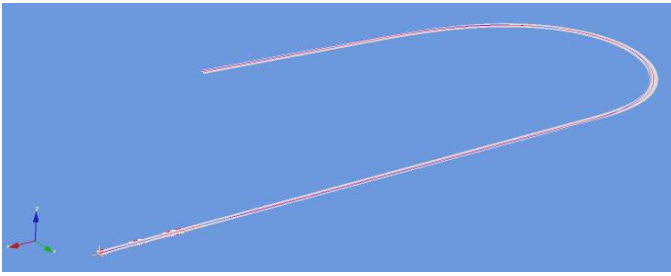


Figure 1 - Specifically developed track "Parabolica"

For this first relatively simple track, it is worth to deepen how VI-Road makes use of the data of length and curvature defined by the user (Table 2). It is important to notice that the notation " $R = 0$ ", used by the software, it is not physically correct to identify the absence of curvature. The correct notation should be " $R \rightarrow \infty$ ".

Table 2 – "Parabolica" track length vs. curvature radius

Track length (L) [m]	Curvature radius (R) [m]
0	0
700	0
800	100
1300	0
1500	0

Considering the data of Table 2, it is possible to identify four track sections:

1. 0 – 700 m: 700 m straight,
2. 700 – 800 m: the curvature radius smoothly decreases to 100 m,
3. 800 – 1300 m: curvature radius smoothly returns to straight,
4. 1300 – 1500 m: 200 m straight.

The result is a corner which tends "to open" in the exit. As the track is composed by a single non-zero curvature value, the software automatically considers it as a single trajectory segment.

### "GRIP Track"

This second closed-loop maneuver "GRIP Track" has been developed with the objective of defining a specific track for lap-time validation, with a complete mix of medium/high-speed corners to enhance the differences in terms of vehicle directional behavior between different aerodynamic solutions (Figure 2). The width is constant and equal to 10 m, while the slope is kept null. Kerbs have been positioned along the track to provide additional information about vehicle suspensions' dynamic response.

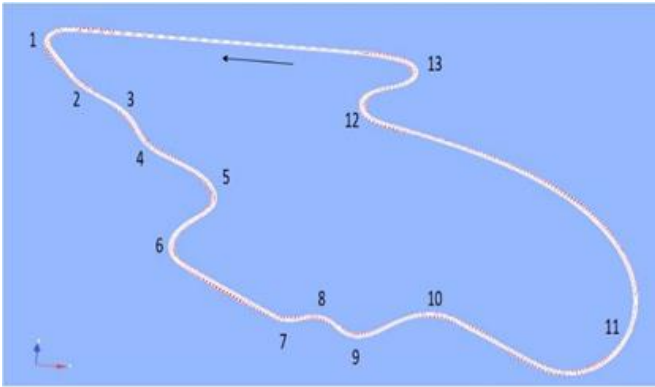


Figure 2 - Specifically developed track "GRIP Track"

In this case, a deeper technical analysis about the trajectory segment splitting performed by the software is necessary in order to define a basic reference system for simulation's results interpretation. For clarity and simplicity purposes, the following "relevant sectors" are defined:

- First corner – First straight and Turn 1
- Fast direction changes – Turn 2, 3, 4, 5
- Turn 6
- Slow direction changes – Turn 7, 8, 9, 10
- "Roundabout" – Turn 11
- Technical part - Turn 12, 13

#### Baseline Aerodynamic and Surfaces Design

Based on the initial CFD analysis of the vehicle body, illustrated in Figure 3, it is possible to note a quite unbalanced downforce distribution with positive downforce on the front axle and negative lift on the front. The resulting aerodynamic forces at 160 km/h are reported in

Table 3.

Considering this information two aerodynamic surfaces have been designed to improve the aerodynamic behavior and allow for the active aerodynamic strategy.

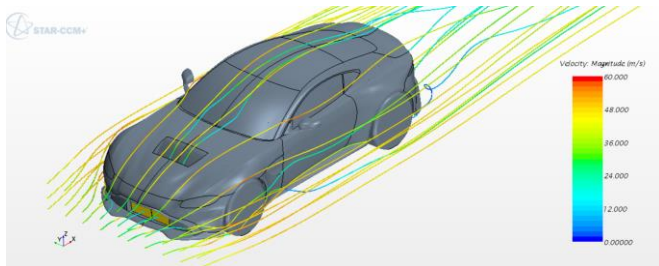


Figure 3 - Reference Vehicle CFD analysis, streamlines

The following targets were provided to the aerodynamic design:

- Implementing an aerodynamic baseline configuration with aerodynamic balance as close as possible to 0.5, increasing downforce in the process, without worsening the aerodynamic efficiency of the vehicle.
- Implementing at least two active surfaces in order to be able to actively modify not only drag and downforce, but also aerodynamic balance in order to have a more impactful control on vehicle stability.

The aerodynamic modifications applied on the reference vehicle (Figure 4) consist in a modified splitter and a rear wing added to the original vehicle, both able to work as active surfaces. The final aerodynamic forces are shown in

Table 3.

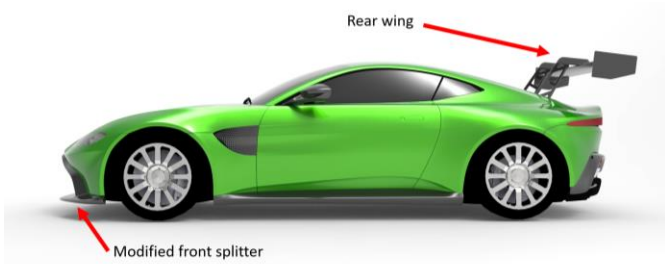


Figure 4 - New reference vehicle aerodynamic interventions

Table 3 – Resulting aerodynamic forces at 160 km/h

Force	Original Vehicle	New Aero Pack
Drag	752 N	788 N
Front Downforce	370 N	470 N
Rear Downforce	-126 N	467 N

To provide a vision of how these aerodynamic modifications affects vehicle dynamics, the new reference vehicle performance has been compared to the original one on GRIP-Track (Figure 5).

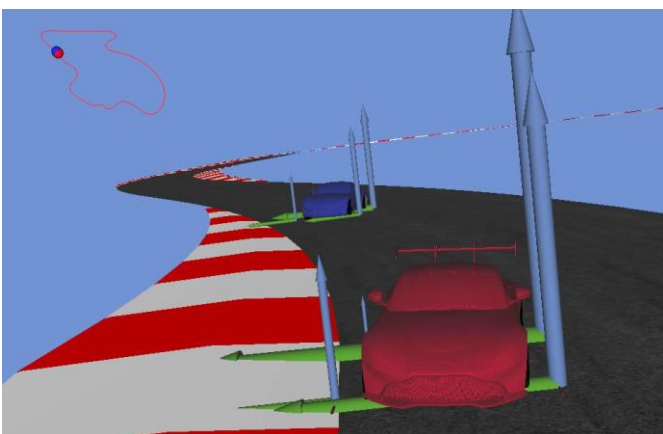


Figure 5 - New aero-pack (red vehicle) validation and original (blue vehicle), GRIP Track

The aerodynamic downforces behavior results much more balanced than on the original reference. Figure 6 shows the comparison aerodynamic balance (defined as the ratio between front downforce ant the total

downforce of the vehicle) of the original vehicle and the new designed aerodynamic pack, throughout a fast lap in the GRIP Track. The variation on the balance is due to the change in pitch and ride height of the vehicles in the lap.

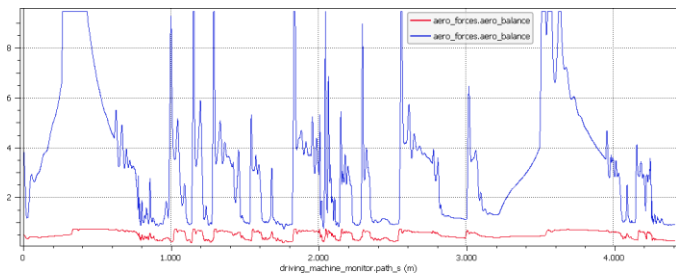


Figure 6 - Aerodynamic balance vs. Track path distance, new aero-pack (red) and original vehicle (blue), GRIP Track

Looking at the speed profiles (Figure 7) however, it is quite clear the advantage that this new aero-pack provides in hard braking and in fast direction changes, where the new vehicle shows a much more stable behavior. However, the new reference vehicle shows to be slower in corner traveling ( $\approx 3$  km/h on average), making so that the original lap-time is 111.251 s while the new model's is 112.258 s

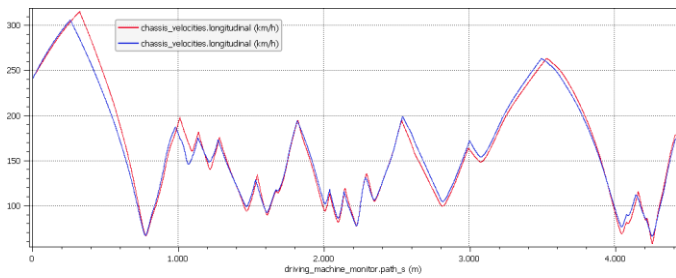


Figure 7 – Longitudinal speed vs. Track path distance, new aero-pack (red) and original vehicle (blue), GRIP Track

One should expect that a more balanced aerodynamic behavior will improve the lap-time, so the authors have hypothesized and tested an explanation to this unintuitive phenomenon.

The explanation rests on the fact that a balanced aerodynamic force distribution is not the best solution if the vehicle chassis is “mechanically” unbalanced. In this case, the vehicle presents an equilibrated mass distribution and a very high torque availability, split equally between front and rear axle. This way, the acceleration phase after the corners create a strong understeering behavior, that was initially counterposed by the forward position of the CoP. Passing to a more balanced aerodynamic configuration, the virtual driver was not able to achieve the same level of exit acceleration, therefore jeopardizing the lap-time.

To verify this explanation, two new configurations were simulated in the GRIP track (Table 4): the first neglects the front motors and rendering the vehicle an RWD (with half power); the second regards a Torque Vectoring logic to apply a Direct Yaw Control strategy and force a neutral behavior [9-11]. Both configurations avoid, mechanically, the issues related to understeering in exit acceleration.

Table 4 – Vehicle balance validation, GRIP Track lap-times summary

Dynamic set-up	Aerodynamic set-up	Time delta
----------------	--------------------	------------

	Original	New	
Standard	111.251	112.258	+ 1.007 s
RWD – Half power	118.530	112.600	- 5.930 s
Torque Vectoring	108.000	106.173	- 1.827 s

From the results presented in Table 4 it is possible to conclude that, indeed, for a mechanically balanced vehicle (Torque Vectoring) or for a vehicle with more pronounced oversteering (RWD) the better aerodynamic balance is beneficial to the lap-time.

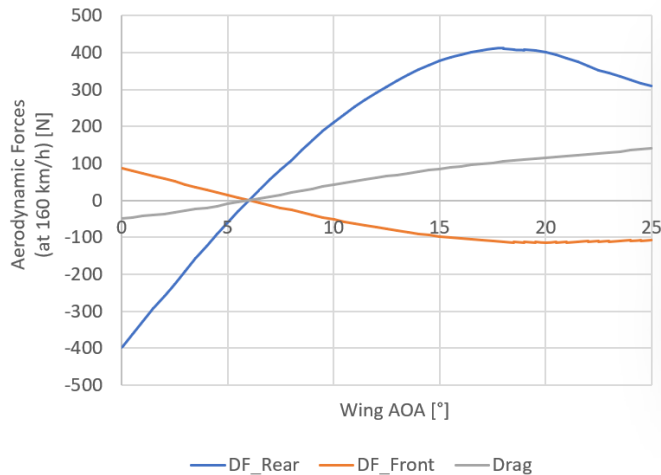


Figure 8 – Active wing Drag (gray) Front downforce (orange) and Rear downforce (blue) vs. Wing Angle of Attack AOA

From the standard configuration it was developed a control strategy to improve the lap-time based on the actuation of two active aerodynamic surfaces:

- Active front splitter: allows for two discrete configurations, closed and open. The former corresponds to the Standard setup, while the later reduces the drag and overall downforce by opening a duct that redirect some of the frontal flow to the underbody.
- Active wing: can be controlled in a continuous actuation operated through mechanical variation of the wing relative Angle of Attack (AOA). Figure 8 shows the aerodynamic forces for each AOA between 0° and 25° referred to the incoming flow. In the Standard setup the AOA is equal to 6°.

#### State machine and Control Strategy

The chosen strategy is the implementation of a state machine high-level control, that receives the inputs coming from the vehicle and translate them into pre-defined state changes in the aero surfaces.

Those changes are executed in MATLAB/Simulink through external forces and a delay, following the linear superimposition hypothesis.

Three different control models were implemented, with increasing degree of complexity:

- Drag Reduction System (DRS);
- DRS + Aerobrake;
- MaxP.

Each model will be presented and discussed in the following sections.

### *Drag Reduction System DRS*

The first idea to improve vehicle performance is to develop a control system able to reduce drag when necessary. The minimum drag configuration corresponds to the opening of the active splitter and AOA of the wing equal to 0°. The conditions for DRS activation are:

- Minimum activation speed threshold.
- Minimum throttle pedal position threshold (70%).
- Maximum lateral acceleration deactivation threshold (1g).

About the first DRS activation condition, the active splitter moves from high downforce to low drag state at 110 km/h, while the active wing linearly reduces its AOA from 6° to 0° in the speed range between 70 and 120 km/h. After 120 km/h, maintained the other conditions, the system remains at a minimum drag configuration.

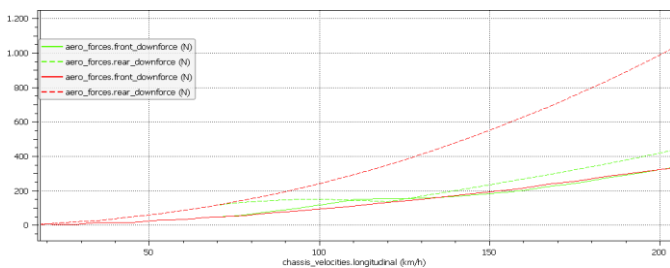


Figure 9 – Downforces vs. speed, Passive (red) and DRS operation (green), straight acceleration

Figure 9 shows the actuation of the system under the DRS logic in a straight full-throttle acceleration. Up to 70 km/h the behavior is equal to the passive, after that a transition phase occurs and a low downforce and low drag state is achieved. As an overall result of the drag reduction the acceleration from 0 to 300 km/h is performed in 10.650 s instead of 10.728 s in the passive configuration.

### *DRS + Aerobrake*

The second step in the state machine development process is to introduce an Aerobrake system. The basic idea is to maximize downforce in braking conditions despite the aerodynamic efficiency. To reach the target, the splitter must stay in high downforce position, as in baseline configuration, and the main aerobrake action can be exerted by increasing the AOA of the rear wing up to 19°.

Similarly, some activation conditions are setup to this configuration:

- Minimum activation speed threshold of 70 km/h.
- Minimum brake pedal position threshold (40%).
- Maximum lateral acceleration deactivation threshold (1g).

To test the control logic and its efficiency, a comparison with the simple DRS system was performed in the 'Parabolica' track.

Figure 10 represents the speed profile of the models and Figure 11 shows the evolution of the aerodynamic drag during the maneuver. It's possible to appreciate the activation of the aerobrake condition once the braking phase starts, increasing the drag force and allowing the driver to delay the deceleration and maintain a slightly higher speed throughout the curve.

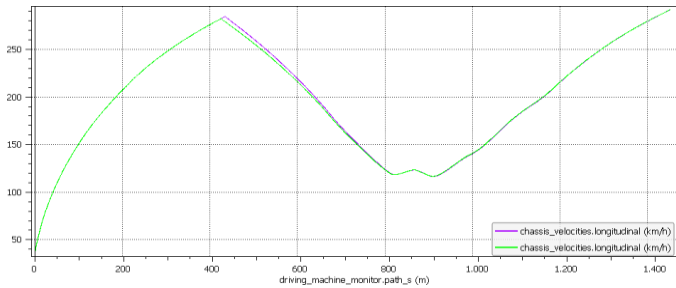


Figure 10 – Speed vs. Track Path, DRS+Aerobrake (purple) and DRS (green), Parabolica

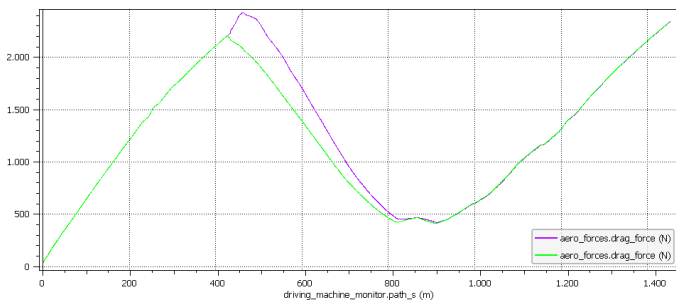


Figure 11 – Drag vs. Track Path, DRS+Aerobrake (purple) and DRS (green), Parabolica

The time to complete the maneuver fall from 29.860 s to 29.791 s in the single corner.

The lap time advantage is also supported by the change in the aerodynamic balance, as in Figure 12. The activation of the aerobrake increases the AOA and dislocate the CoP towards the rear axle, improving the stability and allowing for a higher maximum lateral acceleration.

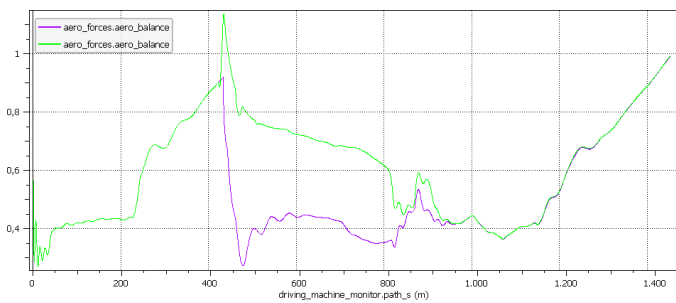


Figure 12 – Aerodynamic Balance vs. Track Path, DRS+Aerobrake (purple) and DRS (green), Parabolica

### MaxP

As a last step in the active aerodynamics control logic, the aerodynamic balance effects on performance are considered. As the overall impact on performance is a sum of different effects, an empirical approach has been

followed to identify the ideal aerodynamic balance as a function of the speed for the Maximum Performance (MaxP) configuration.

To do so, different ramp steering maneuvers has been performed at increasing speed, modifying the wing AOA. The results of this test procedure are reported in Figure 13.

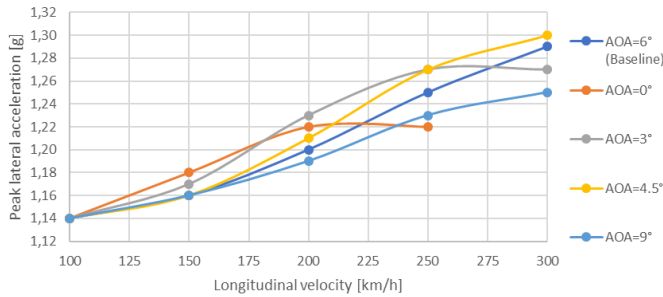


Figure 13 – Peak lateral acceleration vs. Maneuver speed, Different wing AOA, Ramp steering

Differences are noticeable for a vehicle speed higher than 100 km/h. In the range between 100 and 180 km/h, the best aerodynamic configuration is the one with a wing AOA of 0°; AOA of 3° proves to be the best AOA solution from 180 to 250 km/h, while 4.5° appears as best up to 300 km/h.

The baseline configuration - AOA of 6° - never becomes the best in the speed range of interest (even if considering that each aerodynamic configuration seems to follow the same trend, with different scales, probably it would be the best configuration at a speed higher than 300 km/h).

The MaxP algorithm then acts when both DRS and Aerobrake are deactivated, continuously controlling the rear wing AOA according to the results of this analysis.

To verify the improvement proportionated by this additional control logic, tests on the ‘Parabolica’ track were performed and compared with the performance of the DRS+aerobrake set up.

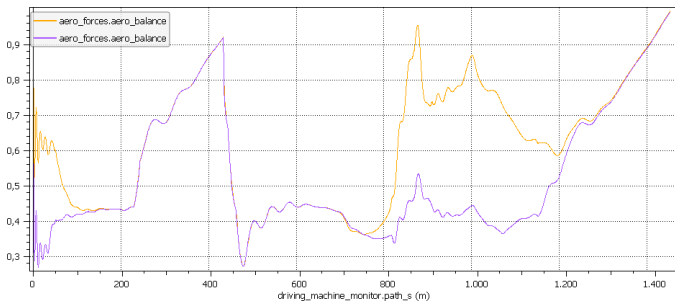


Figure 14 – Aerodynamic Balance vs. Track Path, DRS+Aerobrake (purple) and MaxP (yellow), Parabolica

Referring to Figure 14, MaxP algorithm moves forward the CoP in corner travelling and exiting. The difference in terms of speed profiles has not been reported as it is very subtle, (about 0.3 km/h). The major impact on travelling time is given by the higher precision of the vehicle (represented by the distance from desired path in Figure 15) which allows the VI-Driver to travel a lower distance at a higher speed.

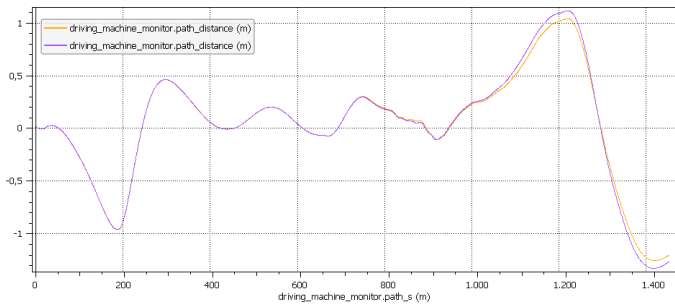


Figure 15 – Distance from desired path vs. Track Path, DRS+Aerobrake (purple) and MaxP (yellow), Parabolica

The improvement in the time to complete the maneuver is an additional 33 ms, making the final time 29.758 s.

### Simulation results and validation

All the developed control algorithms are finally tested on GRIP-Track for validation and performance summary (Table 5).

Table 5 – Active aerodynamics control algorithms, GRIP-Track lap-times

Aerodynamic Configuration	Lap-time [s]
Passive - Original aero pack	111.251
Passive - New aero pack	112.258
DRS	112.260
DRS + Aerobrake	108.414
MaxP	108.137

An interesting observation can be done focusing on what happen in the first segment on the circuit (first straight and first corner), comparing the 2<sup>nd</sup>, the 3<sup>rd</sup> and the 4<sup>th</sup> configurations. Referring to Figure 16 despite a higher top speed reached thanks to DRS activation (around 1km/h), the vehicle seems to be slightly less effective in braking phase with the DRS active.

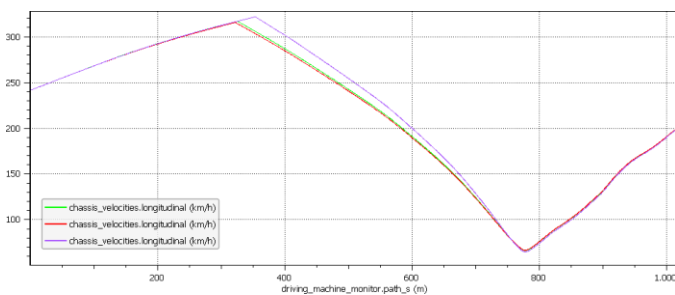


Figure 16 – Speed vs. Track Path, DRS+Aerobrake (purple), DRS (green) and Passive (red), First corner of GRIP-Track

In Figure 17, the 1<sup>st</sup> order filtered actuation of the active wing imply a not negligible delay between when the driver starts braking and when the wing is in baseline position. Observing the lap-time comparison between DRS case and passive-new aero case, it could be said that the time gained on the straight is substantially lost in braking. This effect is clearly compensated by actuating the aerobrake, which seems to be the most effective algorithm in terms of lap-time.

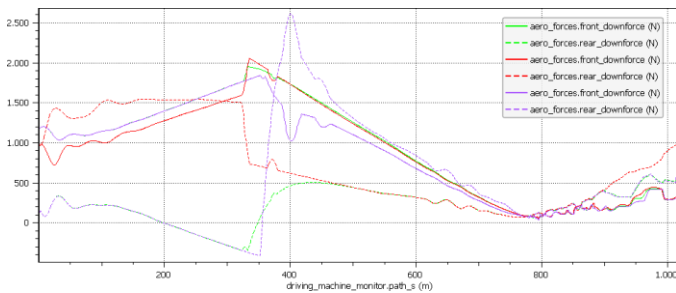


Figure 17 – Front (continuous line) and Rear (dashed line) downforce vs. Track Path, DRS+Aerobrake (purple), DRS (green) and Passive (red), First corner of GRIP-Track

Once that the performance improvement is validated in a track simulation with a virtual driver, the next step is to confirm that the advantages of the active aerodynamic control system would be also useful to a human driver.

To do so, a DIL approach was chosen, due to its ease of implementation and test freedom in comparison with real track testing.

#### *Model Validation on DIL Static Simulator*

The validation was performed in VI-Grade DIL static simulator located in Udine (IT). The static simulator hardware is composed of:

- Steering wheel with active force feed-back;
- Passive pedals;
- Active driving seat provided by pneumatic bags able, by inflating, to reproduce reaction forces exerted by the seat on the driver in occasion of longitudinal (positive) and lateral accelerations;
- Active seat belts able to increase their tension to reproduce reaction force exerted by the belts on the driver in hard braking;
- Shakers positioned below the seat to reproduce high frequency ride vibrations from the road profile or kerbs;
- Curved screen on which the field of view of the driver is projected;
- Sound system;
- Dashboard on the steering wheel for driver information;
- Real-time telemetry to a support computer.

The GRIP-Track was not modelled for the static simulator interface, instead the Nurburgring GP (post-2000) track was selected. The track is comparable with the GRIP-track in terms of speed profiles and lengths, and an important additional input is the presence of kerbs, slopes and asphalt roughness that increase the level of complexity of the track.

Three configurations were tested: Passive system with original aero pack; Passive system with new aero pack and Active system in the MaxP configuration. To better appreciate the improvements, the virtual driver simulations were performed in the same track and its results compared with those of the human driver in the simulator.

The summary of the lap-times is shown in Table 6. Notice that the lap-time improvements are consistent with the ones observed in the GRIP-Track for the virtual driver. The human driver is always slower than the virtual driver (as expected since the virtual driver make no mistakes and iterates to find the optimal solution). In terms of aero configuration, the DIL is able to improve their performance with the evolution of the system in a more pronounced way.

Table 6 – Validation tests, Nurburgring GP best lap-times

Configuration	Virtual	DIL	Delta to previous	
			Virtual	DIL
Passive – Original Aero	115.48 s	134.82 s		
Passive – New Aero	114.08 s	131.61 s	-1.40 s	-3.21 s
Active – MaxP	112.29 s	129.06 s	-1.79 s	-2.55 s

Knowing that the effects of the improved aerodynamics are effective in reducing the lap-time also for a human driver, the attention is turned to the subjective evaluation of the vehicle and its setups, possibly the outcome of most interest in this kind of experiment.

In the following, subjective comments (driver) and additional observations, accompanied by significant telemetry plots, are reported.

#### Passive – Original aerodynamic

The subjective comments from the driver are:

- The car results very unstable in braking. It is very difficult to find the optimal braking point;
- The vehicle suffers strong understeering in corner exiting. It is very easy to completely loose vehicle directionality when opening throttle.

#### Passive – New Aero-pack

The subjective comments from the driver are:

- The vehicle seems more precise in medium-speed corners if compared to the original aerodynamic configuration (noticeable also from the analysis of the downforces in Figure 18 where a much more steady balance and a higher total force is shown)
- It is slightly more understeering in corner traveling, particularly in fast corners, but it can be easily compensated anticipating the trajectory, increasing the steering angle or operating brakes.
- The vehicle appears more stable and effective in braking (As depicted in Figure 19 with later braking points and lower presence of speed fluctuations, that indicate instability)

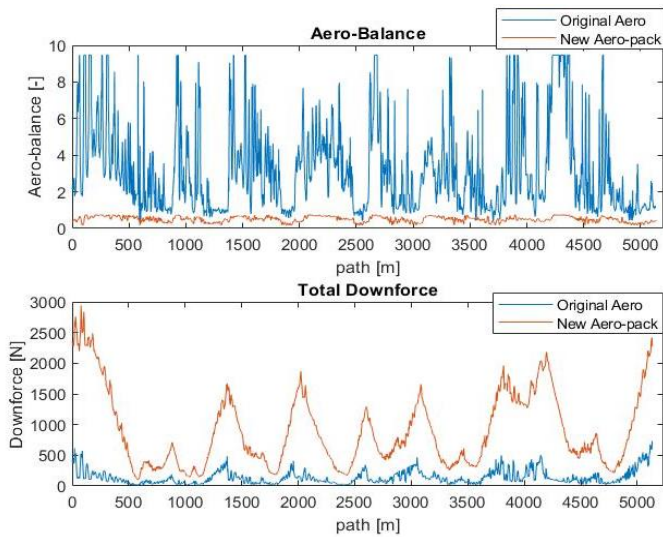


Figure 18 – Aero Balance (top) and total downforce (bottom) vs. Track path, Original aero pack (blue) and New aero pack (orange), DIL simulator

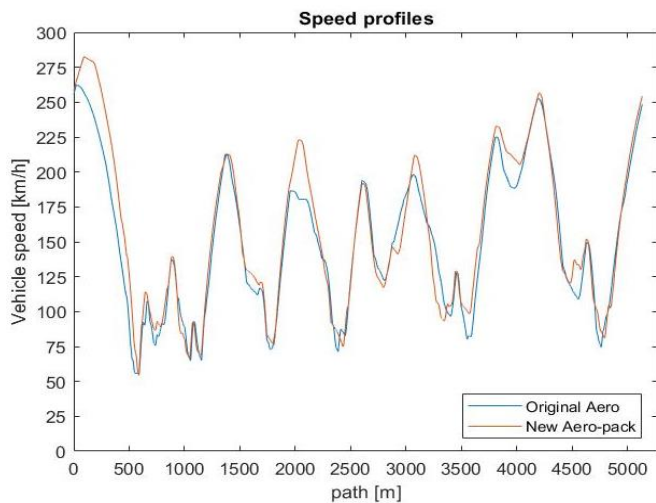


Figure 19 – Speed profile vs. Track path, Original aero pack (blue) and New aero pack (orange), DIL simulator

### Active Aero MaxP

The subjective comments from the driver are:

- The vehicle shows more directionality in all kind of corners.
- The car feels, generally, more precise allowing the driver to face the track more confidently.
- Increased effectiveness in braking. (The effect is appreciable in the speed profile plot in Figure 20)
- The Active Aerodynamic Devices action is visible in Figure 21, both in terms of drag reduction, aerobrake and balance control.

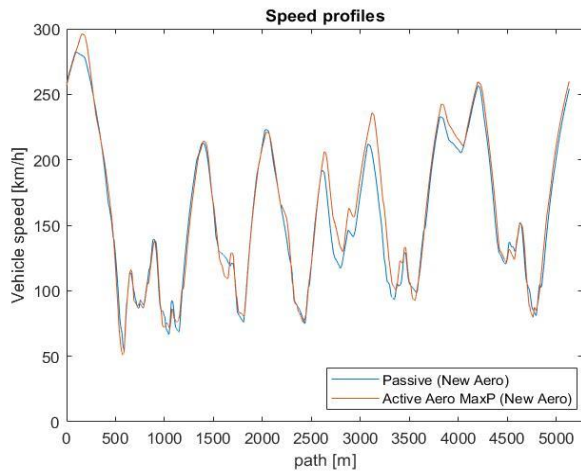


Figure 20 – Speed profile vs. Track path, Passive (blue) and Active MaxP (orange), DIL simulator

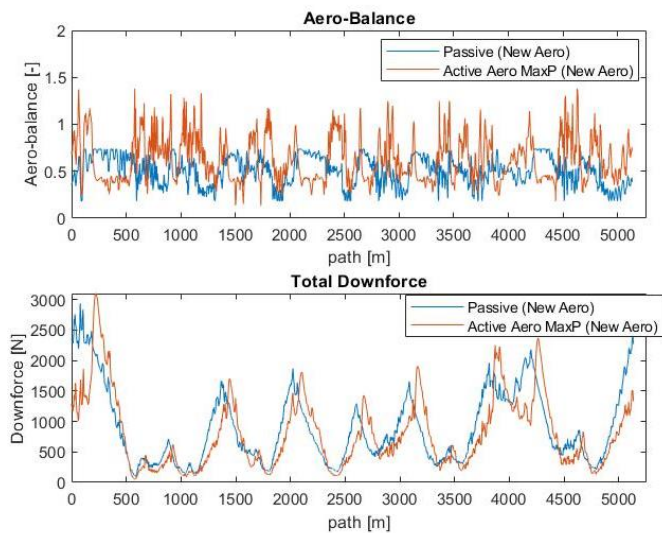


Figure 21 – Aero Balance (top) and total downforce (bottom) vs. Track path, Passive (blue) and Active MaxP (orange), DIL simulator

## Conclusion

The development of a new aero package and the implementation of an active aerodynamics control strategy were successful in the proposed case study of an electric hyper car in terms of lap-time reduction.

One important insight emerged when the reference vehicle original aerodynamic configuration has been compared to a new aero pack specifically developed to increase overall downforce, distributing it in an almost perfectly balanced way between front and rear axles. It has been demonstrated, both empirically and theoretically, that a perfectly balanced aerodynamics is not the best possible solution for a “mechanically unbalanced” vehicle and that it is not possible to fully exploit the potential advantage given by the total downforce, if the vehicle is not balanced and neutral behaving. For these reasons, the same prioritization method was used to dynamically adjust the vehicle aerodynamic balance in order to keep the best possible handling behavior and vehicle overall balance at every speed and driving condition.

After that, the high-level control logic based on aerodynamic state variation, commanded by inputs coming from the vehicle (such as speed, driver inputs and acceleration) proved to be easy to implement and effective in improving the overall performance of the vehicle in the track.

One of the most interesting points of the presented study is the validation of the performance improvement in the DIL simulator. It has been demonstrated that the active system is appreciable also for a human driver, and more than that, the improvements are higher than the ones seen for the virtual driver. The general explanation lays on the fact that the human driver suffers more with unstable and unpredictable driving conditions (as was evaluated the original configuration) and the new aero pack and its control logic help on increasing the total downforce and correcting the fluctuations on the aerodynamic balance, rendering the driving experience much more intuitive.

Future developments include the experimental validation of the results with a real vehicle in a track test, the integration of the active aero dynamics system with other kinds of control algorithms (such as Torque Vectoring or Active suspensions) and the improvement of the virtual driver logic to match more accurately the results of a human driver.

## References

1. Ferraris A., Airale A. G., Berti Polato D., Messana A. et al., "City Car Drag Reduction by Means of Shape Optimization and Add-On Devices". *Advances in Mechanism and Machine Science IFToMM WC 2019. Mechanisms and Machine Science*, vol 73. Springer, 2019. doi: [10.1007/978-3-030-20131-9\\_367](https://doi.org/10.1007/978-3-030-20131-9_367).
2. Janson T. and Piechna J., "Numerical analysis of aerodynamic characteristics of a high-speed car with movable bodywork elements", *Vol. LXII, 2015, No. 4*, pp. 451-476. 2015.
3. Diasinos S., Barber T. and Doig G., "Numerical Analysis of the Effect of the Change in the Ride Height on the Aerodynamic Front Wing–Wheel Interactions of a Racing Car". *Proceedings of the Institution of Mechanical Engineers, Part D: Journal of Automobile Engineering* 231, no. 7, pp: 900–914. 2017. doi:[10.1177/0954407017700372](https://doi.org/10.1177/0954407017700372).
4. Vdovin A., Lennart L., Sebben S. and Walker T., "Investigation of vehicle ride height and wheel position influence on the aerodynamic forces of ground vehicles". *The International Vehicle Aerodynamics Conference 2014*, pp. 81-90. 2014. doi:[10.1533/9780081002452.3.81](https://doi.org/10.1533/9780081002452.3.81).
5. Schnepf B., Tesch G. and Indinger T., "On the Influence of Ride Height Changes on the Aerodynamic Performance of Wheel Designs". *JSAE Annual Congress*, 2014.
6. Xu S., Ferraris A., Airale A.G. and Carello M. "Elasto-kinematics design of an innovative composite material suspension system". *Mech. Sci.* 8, 11–22. 2017. doi:[10.5194/ms-8-11-2017](https://doi.org/10.5194/ms-8-11-2017).
7. de Carvalho Pinheiro H., Messana A., Sisca L., Ferraris A., et al. "Computational Analysis of Body Stiffness Influence on the Dynamics of Light Commercial Vehicles". *Advances in Mechanism and Machine Science. IFToMM WC 2019. Mechanisms and Machine Science*, Springer, vol 73. pp. 3117-3126, 2019, doi:[10.1007/978-3-030-20131-9\\_307](https://doi.org/10.1007/978-3-030-20131-9_307)
8. K. Kurec, M. Remer, J. Broniszewski, P. Bibik, S. Tudruj, J. Piechna. "Advanced Modelling and Simulation of Vehicle Active Aerodynamic Safety", *Hindawi, Journal of Advanced Transportation*, 2019. doi:[10.1155/2019/7308590](https://doi.org/10.1155/2019/7308590)
9. de Carvalho Pinheiro H., Messana A., Sisca L., Ferraris A., et al. "Torque Vectoring in Electric Vehicles with In-wheel Motors". *Advances in Mechanism and Machine Science. IFToMM WC 2019. Mechanisms and Machine Science*, Springer, vol 73. pp. 3127-3136. 2019. doi:[10.1007/978-3-030-20131-9\\_308](https://doi.org/10.1007/978-3-030-20131-9_308).
10. de Carvalho Pinheiro H., Galanzino E., Messana A., Sisca L., et al. "All-wheel drive electric vehicle modelling and performance optimization". *SAE Technical Paper 2019-36-0197*, 2020. doi:[10.4271/2019-36-0197](https://doi.org/10.4271/2019-36-0197)
11. Ferraris A., de Carvalho Pinheiro H., E. Galanzino, Airale A.G., et al. "All-Wheel Drive Electric Vehicle Performance Optimization: From Modelling to Subjective Evaluation on a Static Simulator". *Electric Vehicles International Conference, EV 2019. Electric Vehicle International Conference & Show*, 3-4 october 2019, doi:[10.1109/EV.2019.8893027](https://doi.org/10.1109/EV.2019.8893027).

12. de Carvalho Pinheiro H., Russo F., Sisca L., Messina A., et al. "Advanced vehicle dynamics through active aerodynamics and active body control". Proceedings of the ASME 2020 International Design Engineering Technical Conferences and Computers and Information in Engineering Conference, IDETC2020. St. Louis, MO, USA. 2020. To be published.
13. de Carvalho Pinheiro H., Russo F., Sisca L., Messina A., et al. "Active aerodynamics through active body control: modelling and static simulator validation". Proceedings of the ASME 2020 International Design Engineering Technical Conferences and Computers and Information in Engineering Conference, IDETC2020. St. Louis, MO, USA. 2020. To be published.
14. de Cupis D., de Carvalho Pinheiro H., Ferraris A., Airale A.G., et al. "Active Aerodynamics Design Methodology for Vehicle Dynamics Enhancement". Advances in Mechanism and Machine Science, Proceedings of 3rd IFToMM ITALY Conference, IFIT 2020. Napoli, Italy, 2020. To be published.

## Contact Information

Politecnico di Torino – Department of Mechanical and Aerospace Engineering  
C.so Duca degli Abruzzi, 24 -10129 Torino – Italy  
Phone: +39.011.0906946

Massimiliana Carello  
massimiliana.carello@polito.it

Alessandro Ferraris  
alessandro.ferraris@polito.it

Davide de Cupis  
s250289@studenti.polito.it

Henrique de Carvalho Pinheiro  
henrique.decarvalho@polito.it

Alessandro Messina  
alessandro.messana@polito.it

Lorenzo Sisca  
lorenzo.sisca@polito.it

Andrea Giancarlo Airale  
andrea.airale@polito.it

## Acknowledgments

The authors wish to acknowledge all the VI-grade Italy Team, for the software and help in the activities.

## Definitions/Abbreviations

4WD	Four Wheels Drive
AOA	Angle Of Attack
CAD	Computer Aided Design
CFD	Computational Fluid Dynamics

CoG	Center of Gravity
CoP	Center of Pressure
DIL	Driver In the Loop
DOF	Degrees Of Freedom
DRS	Drag Reduction System
RWD	Rear Wheels Drive